Journal of Ceramic Processing Research. Vol. 22, No. 3, pp. 345~355 (2021)
(Received 3 November 2020, Received in revised form 9 February 2021, Accepted 2 March 2021)
https://doi.org/10.36410/jcpr.2021.22.3.345

J O U R N A L O F
Ceramic Processing Research

Minimization of delamination, surface roughness and thrust force in drilling of Al_2O_3 ceramic particle filled CFRP composites

M. Srinivasan[a,*], S. Ramesh[b], S. Sundaram[c] and R. Viswanathan[d]
[a]*Research Scholar, Anna University Chennai, India*
[b]*Department of Mechanical Engineering, School of Engineering, Presidency University, Bengaluru, India*
[c]*Department of Mechanical Engineering, Muthayammal Engineering College, Rasipuram, India*
[d]*Department of Mechanical Engineering, AVS Engineering College, Salem, India*

Present study explores the influence of filler material and drilling parameters on delamination factors, surface roughness and thrust force in the drilling of carbon fiber reinforced epoxy composites (CFRP) using high speed steel (HSS) drill. The CFRP composite was fabricated by hand layup technique and the drilling tests were carried out using L27 orthogonal array (OA) design with wt% of Al_2O_3, spindle speed, point angle and feed rate as input process parameters. Grey Relational Analysis (GRA) is used for multi objective optimization and optimum parameter condition obtained include 4 wt% of Al_2O_3, 3000 rpm speed, 100° point angle and 50 mm/min feed. The optimum set of inputs resulted in 1.1469 and 1.2918 as entry and exit delamination factor values, 1.94 µm surface roughness and 95.29N thrust force. ANOVA is employed to find the influence of process variables on output responses.

Keywords: Composites, grey relational analysis, ANOVA, drilling, optimization.

Introduction

The reasons for the industrial developments in the past few decades could be attributed to the development of new and modern manufacturing methods. Among the new materials that have come to stay, composites occupy almost all the fields such as automobile, aero-space, defence, biomaterials and sports. These materials, once primarily manufactured for aerospace applications, have now become a part of our day-to-day life products.

Drilling is one of the most essential processes in the development of different structures and components for the aeronautical industry as large number of drilled holes are required in the fabrication process. Drilling of composites, particularly CFRP composites is a challenging task. The main problems that arise in the drilling of CFRP include increased amount of delamination, surface roughness, thrust force and tool wear [1]. Almost 60% of the parts get rejected for defects in the aircraft industry due to inappropriate selection of drilling parameters [2]. Therefore selection of appropriate machining parameters is essential for reducing defects that arise while drilling operations, especially composites that contain heterogeneous mix of materials. Researchers [3-5] have revealed that damages like peel-up at the entrance and push-down at the exit of the hole could occur. Past studies also state that occurrence of delamination increases with the increase in feed rate, though delamination is found to diminish with an increase in cutting speed [6, 7].

Ricardo et al. [8] have reinforced 7.5, 10 and 11.5 wt% of graphite in the epoxy to study the performance and found the enhancement of mechanical properties up to a limiting value of graphite reinforcement and subsequently the performance got reduced due to graphite agglomeration in the matrix. Rajmohan [9] studied the effect of inclusion of fly ash filler material into CFRP composites and concluded that the addition of fly ash reduced delamination damage.

Ranganatha & Ramamurthy [10] analysed the effect of incorporartion of Al_2O_3 on the mechanical properties of CFRP and observed remarkable progress in the impact strength with the increase in the alumina reinforcement up to 4% and showed reducing trend for 6% alumina inclusion. Krishnaraj et al. [11] reported that feed rate had a dominant effect on push-out delamination, thrust force and hole diameter in the drilling of CFRP laminates with K20 carbide drill. Zhang et al. [12] have stated that main damage mechanisms that occur at exit are produced by spalling and fuzzing and also these damages increase with decrease in spindle speed and increase in feed rate in the drilling of unidirectional and multi-directional CFRP laminates by HSS twist drill.

Heisel et al. [13] noticed that quality of the drill hole at the entrance could be improved with increasing point

*Corresponding author:
Tel : ++919443084485
E-mail: m75sri@gmail.com

angle and increasing feed forces as well, but the exit hole quality remained poor. Durao et al. [14] revealed that surface quality could be improved a little by increasing the feed, whereas no clear influence of the cutting speed was detected.

Krishnamoorthy et al. [15] have reported feed rate as the most influencing controlling factor on multiple performance characteristics followed by spindle speed and point angle in drilling of CFRP composite plates by using Grey-Fuzzy optimization. Aravind et al. [16] applied Taguchi –GRA approach to lower the delamination factor and also simultaneously increase the MRR in the micro drilling of CFRP laminates. Abhishek et al. [17] have achieved lowest torque, thrust, and delamination factor (entry & exit) by applying lowest feed, maximum drill speed and lowest drill diameter through PCA-Fuzzy-Taguchi optimization method. Researchers [18-21] have also effectively employed taguchi based GRA technique on multi objective optimization to obtain optimal parameters.

The review of literature provided the gap and scope for the author to study effect of the machining parameters on thrust force, roughness and delamination during the drilling of Al_2O_3 filled CFRP composites. It has also been noticed that adequate investigations have not been carried out to find the effect of drilling parameters on multi responses during the drilling of Al_2O_3 filled CFRP composites. This is significant because these factors play an important role in the performance of the machined component. Thus, the study presents the results of a detailed experimental investigation to determine the effect of cutting parameters in drilling CFRP composites.

Materials and Methods

In the present work, carbon fiber of 600 GSM grade woven rowing material was used and its specifications are presented in Table 1. The fiber weight fraction was fixed as 40% with bi-directional orientation. Epoxy resin grade of LY556 was used with Hardner HY951 to form composite plate and the important properties of these materials are presented in Table 2. The mixing ratios of resin and hardener utilized for the work are shown in Table 3.

In the first step of fabrication, the Al_2O_3 nanoparticles were dispersed into acetone and mixed with the epoxy. Specifications of the Al_2O_3 powder are presented in Table 4. The mixtures thus prepared in different proportions were stirred with Ultrasonic cavitations (60% amplitude for about 30 min). In the next step, acetone was removed from the epoxy mixture by using vacuum oven (70 °C for 24 h). Lastly, the curing agent was added manually into the epoxy and stirred for 5-7 min. Then the uniform mixture of epoxy resin was applied on the carbon fiber surface. Slight pressure was applied on to the surface using a roller, to remove any air trapped as well as the surplus polymer present. Each laminate was cured for 24 h by hydraulic press under a pressure of 30 bar. The prepared composite was cut into sizes of 150 × 60 mm plates with a thickness of 3 mm.

The drilling operations were carried out in the CNC vertical machining center - ARIX VMC 100 under dry conditions using HSS twist drill. The drilling parameters used in the study are provided in Table 5. In this work, L27 OA design was utilized to conduct the drilling experiments on the plates. The holes were photographed using CANON EOS 5D Mark III camera and the digital images analysed using CORELDRAW software. Ra and thrust force were measured by Mitutoyo surface roughness tester (Model: Surftest-211) and dynamometer (Kistler-9257B type) respectively and the instruments are shown in Fig. 1. And Table 6 presents the measured output responses. Delamination factor was calculated using the formula given below [22].

Table 1. Bidirectional carbon fiber- mechanical properties

Grade (GSM)	600
Diameter of carbon fiber	8 μm
Filament Tensile strength	4.133 GPa
Filament Tensile modulus	234 GPa
Density	1.70 g/cm^3

Table 2. Resin and hardener property

Property	Unit	Araldite LY 556	Aradur HY 951
Viscosity at 25°C	mPa.s	10,000-12,000	10 - 20
Density at 25°C	gm/cc	1.15-1.20	0.97-0.99
Flash point	°C	> 200	>180

Table 3. Resin and hardener - Mixing ratio

Material	Part by weight
Araldite LY 556	100
Aradur HY 951	10-12

Table 4. Specifications of Al_2O_3 filler material

Property	Value
Particle Size	40 nm
Density	3.987 g/cm^3
Young's modulus	215 GPa
Poisson's ratio	0.21
Tensile strength	665 MPa
Compressive strength	5500 MPa

Table 5. Drilling conditions

Parameters	Symbol	Level 1	Level 2	Level 3
Spindle Speed, RPM	V	1000	2000	3000
Point angle, degree	θ	100	118	135
Feed rate, mm/min	f	50	100	150
Wt% of Al_2O_3	A	0	2	4

Table 6. L27 OA & measured output responses

Trial No.	Input parameters				Output responses			
	V (RPM)	θ (degree)	F (mm/min)	A	Delamination Factor		Surface Roughness (Ra) μm	Thrust force (F), N
					Entry	Exit		
1	1000	100	50	0	1.4207	1.4289	1.49	59.814
2	1000	100	100	2	1.3310	1.5486	2.35	87.8864
3	1000	100	150	4	1.2717	1.5981	3.63	158.29
4	1000	118	50	4	1.2509	1.4304	2.98	187.03
5	1000	118	100	0	1.5136	1.7737	2.06	101.316
6	1000	118	150	2	1.4381	1.6756	4.81	165.17
7	1000	135	50	2	1.3268	1.5344	2.06	124.033
8	1000	135	100	4	1.2895	1.5506	3.96	208.46
9	1000	135	150	0	1.5741	1.875	3.53	124.024
10	2000	100	50	2	1.2767	1.3096	1.48	70.9402
11	2000	100	100	4	1.2162	1.3329	2.49	112.76
12	2000	100	150	0	1.4992	1.7325	1.49	77.148
13	2000	118	50	0	1.4527	1.484	1.63	84.108
14	2000	118	100	2	1.3550	1.6490	2.81	118.538
15	2000	118	150	4	1.2726	1.5749	3.94	199.01
16	2000	135	50	4	1.2076	1.2535	2.15	165.56
17	2000	135	100	0	1.5115	1.8463	2.78	93.912
18	2000	135	150	2	1.3972	1.7082	3.79	153.18
19	3000	100	50	4	1.1474	1.2920	1.92	95.26
20	3000	100	100	0	1.4659	1.5879	1.22	58.556
21	3000	100	150	2	1.3379	1.5571	2.40	86.2212
22	3000	118	50	2	1.2920	1.3463	1.45	101.884
23	3000	118	100	4	1.2051	1.4342	3.05	144.66
24	3000	118	150	0	1.5272	1.8628	1.75	108.156
25	3000	135	50	0	1.4566	1.4908	1.99	86.184
26	3000	135	100	2	1.3550	1.6251	2.77	117.536
27	3000	135	150	4	1.2502	1.5659	4.31	213.38

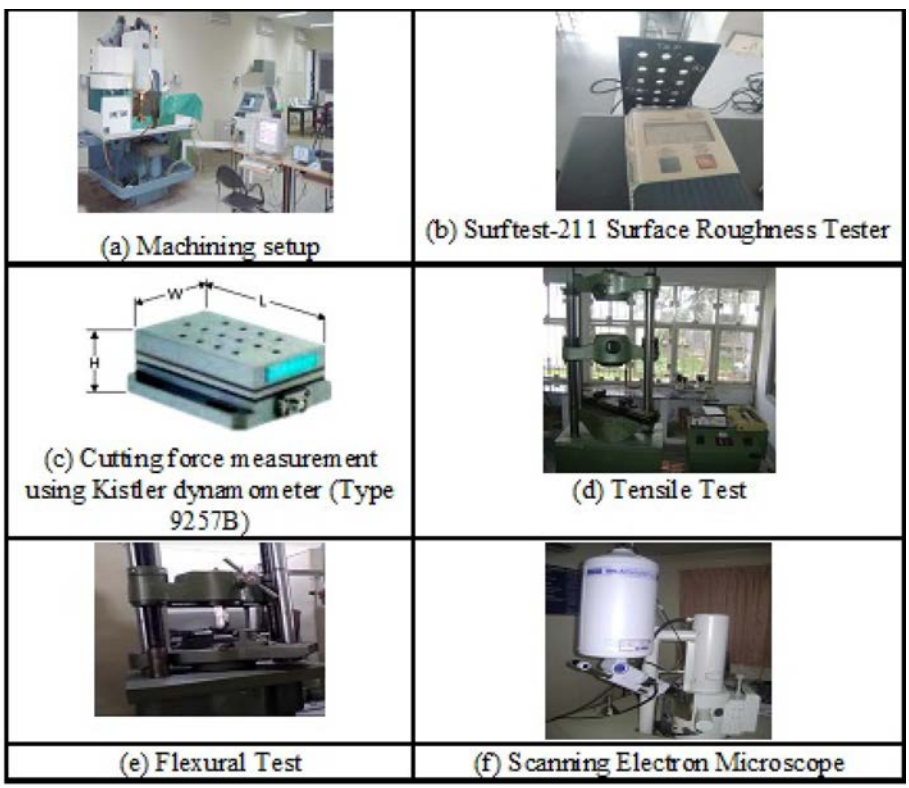

Fig. 1. Experimental setup and measurement of responses.

$$\text{Delamination factor} = \frac{D_{max}}{D_{actual}} \quad (1)$$

Where, D_{max} is damaged diameter around the hole, D_{actual} is actual diameter to be drilled.

Optimization Methodology

Taguchi based GRA is used to define the optimal drilling parameter combination for lower D-entry, D-exit, Ra and F in the drilling of CFRP [23]. The procedure of GRA is as follows [24]:

Initially the measured responses are normalized in the range of zero to one. In this study the considered responses have to be minimized, hence 'the lower the better' characteristic is used and specified as Equation (2)

$$Y_i^*(k) = \frac{\max Y_i^o(k) - Y_i^o(k)}{\max Y_i^o(k) - \min Y_i^o(k)} \quad (2)$$

where $Y_i^*(k)$ - normalized data, $Y_i^o(k)$ - original sequence, $\max Y_i^o(k)$ - greatest value of $Y_i^o(k)$, and $\min Y_i^o(k)$ - lowest value of $Y_i^o(k)$.

The grey relational coefficient (GRC) indicates the relation between the ideal and real experimental results. GRC is denoted as:

$$\xi(k) = \frac{\min_j \min_k \left|Y_o(k) - Y_j(k)\right| + \zeta \max_j \max_k \left|Y_o(k) - Y_j(k)\right|}{\left|Y_o(k) - Y_j(k)\right| + \zeta \max_j \max_k \left|Y_o(k) - Y_j(k)\right|} \quad (3)$$

Where,

Distinguishing coefficient ζ is considered to be 0.5. The grey relational grade (GRG) was calculated by averaging the GRC equivalent to each feature. The GRG can be indicated as:

$$\gamma_i = \frac{1}{n}\sum_{k=1}^{n} \varepsilon_i(k) \quad (4)$$

here, n is no. of responses.

Result and Discussion

Multi objective optimization

The aim of the optimization work is to minimize the D-Entry, D-Exit, Ra and F using Taguchi based GRA technique. Normalization values were calculated using Equation (2) and its plot is shown in Table 7. Equation

Table 7. Normalization, GRC and GRG

S.No	Normalization				GRC				GRG
	D-entry	D-exit	Ra	F	D-entry	D-exit	Ra	F	
1	0.360	0.718	0.925	0.992	0.438	0.639	0.869	0.984	0.733
2	0.570	0.525	0.685	0.811	0.537	0.513	0.614	0.725	0.597
3	0.709	0.446	0.329	0.356	0.632	0.474	0.427	0.437	0.492
4	0.757	0.715	0.510	0.170	0.673	0.637	0.505	0.376	0.548
5	0.142	0.163	0.766	0.724	0.368	0.374	0.681	0.644	0.517
6	0.319	0.321	0.000	0.311	0.423	0.424	0.333	0.421	0.400
7	0.580	0.548	0.766	0.577	0.543	0.525	0.681	0.542	0.573
8	0.667	0.522	0.237	0.032	0.600	0.511	0.396	0.341	0.462
9	0.000	0.000	0.357	0.577	0.333	0.333	0.437	0.542	0.411
10	0.697	0.910	0.928	0.920	0.623	0.847	0.873	0.862	0.801
11	0.839	0.872	0.646	0.650	0.756	0.796	0.586	0.588	0.682
12	0.176	0.229	0.925	0.880	0.378	0.393	0.869	0.806	0.612
13	0.285	0.629	0.886	0.835	0.411	0.574	0.814	0.752	0.638
14	0.513	0.364	0.557	0.613	0.507	0.440	0.530	0.563	0.510
15	0.707	0.483	0.242	0.093	0.630	0.492	0.398	0.355	0.469
16	0.859	1.000	0.741	0.309	0.780	1.000	0.659	0.420	0.715
17	0.147	0.046	0.565	0.772	0.369	0.344	0.535	0.686	0.484
18	0.415	0.268	0.284	0.389	0.461	0.406	0.411	0.450	0.432
19	1.000	0.938	0.805	0.763	1.000	0.890	0.719	0.678	0.822
20	0.254	0.462	1.000	1.000	0.401	0.482	1.000	1.000	0.721
21	0.554	0.512	0.671	0.821	0.528	0.506	0.603	0.737	0.594
22	0.661	0.851	0.936	0.720	0.596	0.770	0.886	0.641	0.723
23	0.865	0.709	0.490	0.444	0.787	0.632	0.495	0.473	0.597
24	0.110	0.020	0.852	0.680	0.360	0.338	0.772	0.609	0.520
25	0.275	0.618	0.786	0.822	0.408	0.567	0.700	0.737	0.603
26	0.513	0.402	0.568	0.619	0.507	0.455	0.537	0.568	0.517
27	0.759	0.497	0.139	0.000	0.675	0.499	0.367	0.333	0.469

(3) is used to compute the GRC values for all the output responses and presented in Table 7. Lastly the grey relational grade (GRG) was assessed by averaging the sum of GRCs by using Equation (4) and the values obtained are given in Table 4. The greater the GRG, it indicates that the quality characteristics are better. Trail 19 has the highest GRG value of 0.822 and it is the best multiple output response among the 27 runs [25].

Based on the GRG response table (Table 8), the feed rate is found to be the foremost dominant factor on multiple performances followed by point angle, spindle speed and wt% of Al_2O_3. Consequently it was revealed that the drilling conditions of 3000 rpm spindle speed, 100° point angle, 50 mm/min (f) and 4 wt% of Al_2O_3 provide the optimal combination for drilling of CFRP composites. The main effects plot in Fig. 2 represents this.

Table 9 indicates the validation experiment details and it assures that the results achieved through optimum set are better than that of trial results attained for the different combinations of input factors. Confirmation experiment illustrates that D-Entry is lowered from 1.2717 to 1.1469, D-Exit is decreased from 1.5981 to 1.2918, Ra is significantly reduced from 3.63 to 1.94 µm and thrust force is reduced from 158.29 N to 95.29 N by applying optimal combination. From the results, it is evident that multi objective optimization can be significantly simplified using this approach. Fig. 3(a) & (b) reveal the images of drilled holes at initial and optimum conditions. It is obvious from Fig. 3(b), that its delamination is lower than that of Fig 3(a).

The predicted GRG can be estimated by using the below equation [31]:

$$\hat{\eta} = \eta_m + \sum_{i=1}^{n} (\overline{\eta}_i - \eta_m) \quad (5)$$

Where η_m is total mean of GRG, $\overline{\eta}$ is optimal level in each response

From the analysis of the results of this multi-objective system (from ANOVA Table 10), feed rate is found to be the most influential factor followed by

Table 8. Response Table for GRG

Level	V	θ	f	A
1	0.5260	0.6726	0.6839	0.5820
2	0.5935	0.5469	0.5651	0.5719
3	0.6183	0.5183	0.4887	0.5839
Delta	0.0923	0.1543	0.1952	0.0119
Rank	3	2	1	4

Table 9. Validation test

	Primary drilling conditions	Optimal drilling conditions	
		Prediction	Experiment
Setting level	$V_1\theta_1f_3A_3$	$V_3\theta_1f_1A_3$	$V_3\theta_1f_1A_3$
D-Entry	1.2717	--	1.1469
D-Exit	1.5981	--	1.2918
Ra (µm)	3.63	--	1.94
F (N)	158.29	--	95.29
GRG	0.492	0.822	0.825
Progress in GRG = **0.333**			

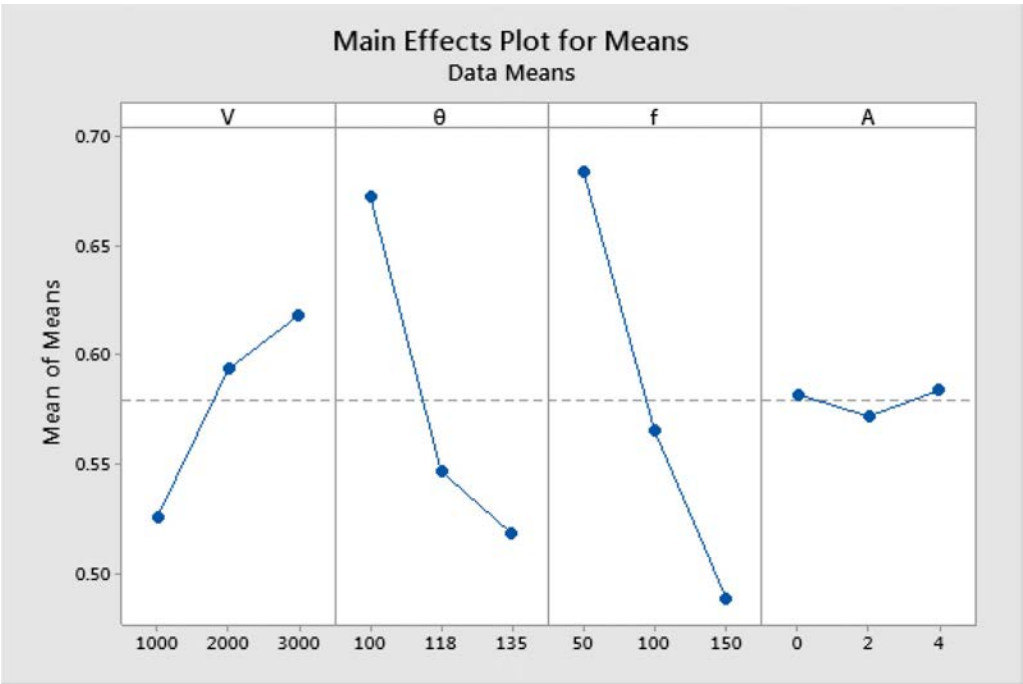

Fig. 2. Main effect plot for GRG

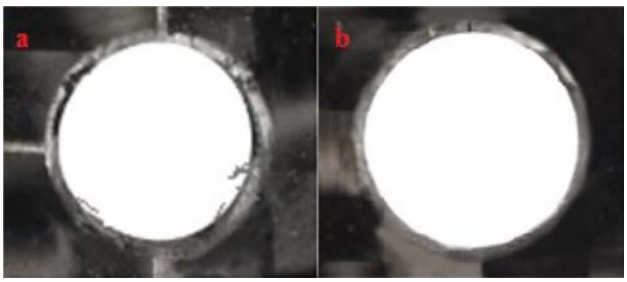

Fig. 3. Drilled hole at initial and optimal condition.

point angle and spindle speed.

Effect of drilling parameters on responses

Figs. 4, 5, 6, and 7 denote the main effect plots for D-Entry, D-Exit, Ra and F respectively. The maximum S/N ratio of factor level assures the best conditions. Consequently it is noted from Fig. 4 and 5 that spindle speed at 3000 rpm, point angle at 100°, feed rate at 50 mm/min and incorporation of 4 wt% Al_2O_3 are the optimal conditions for obtaining lesser D-entry and D-exit. Fig. 4 & 5 also reveal that the D-entry and D-exit holes get enlarged with increase in feed rate while it gets decreased with raise in wt% of Al_2O_3. But spindle speed at 3000 rpm, point angle at 100°, feed rate at 50 mm/min and without incorporation of Al_2O_3 are found to be better combination to achieve lowest surface roughness and cutting force as exposed in Fig. 6 and 7.

During the drilling of Hybrid CFRP composites, the force generated in the opposite direction of the drill results in separating each lamina from the other and thus produces the delaminated zone in the composite. This effect can be decreased by reducing the thrust force caused during drilling. Fig. 8 shows the micrograph of the drilled surface (at a magnification of 500×), in which the fractured fibers in the drilled surface of the composite can be seen clearly.

Analysis of variance

ANOVA is employed to find the significance and effect of each factor on D-Entry, D-Exit, Ra and F [30]. From the analysis, it was observed that reinforcement wt.% has the maximum influence on D-entry (84.92%).

Table 10. ANOVA for GRG

Source	DF	Adj SS	Adj MS	F-Value	P-Value	% of contribution
V	2	0.041075	0.020537	15.51	0.000	11.37
θ	2	0.121262	0.060631	45.79	0.000	33.58
f	2	0.174241	0.087120	65.79	0.000	48.25
A	2	0.000738	0.000369	0.28	0.760	0.20
Error	18	0.023836	0.001324			6.60
Total	26	0.361151				100

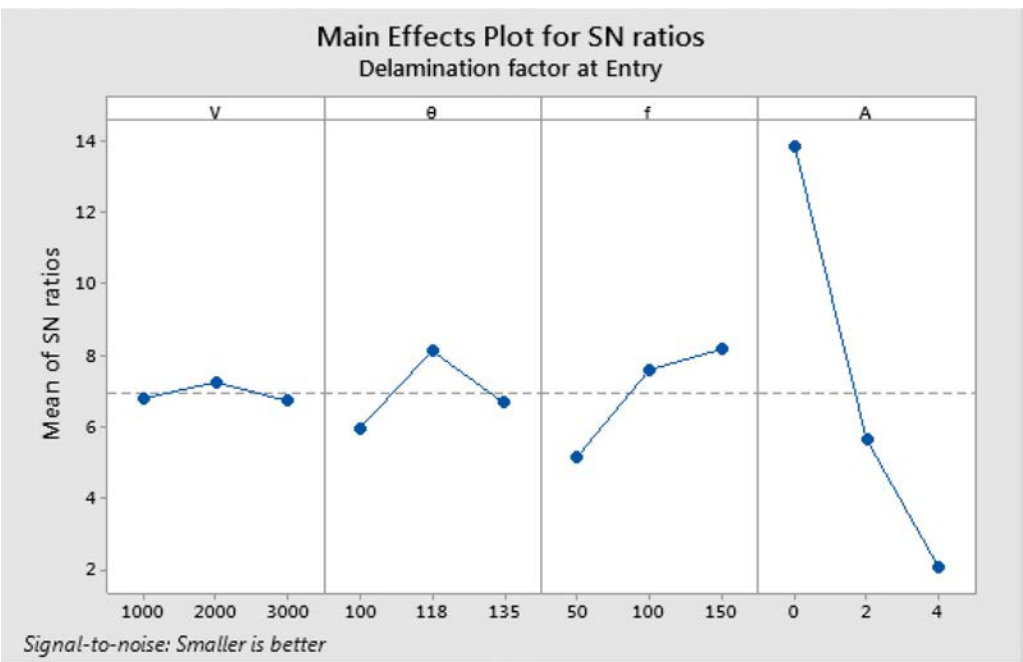

Fig. 4. S/N ratio plot for D-Entry.

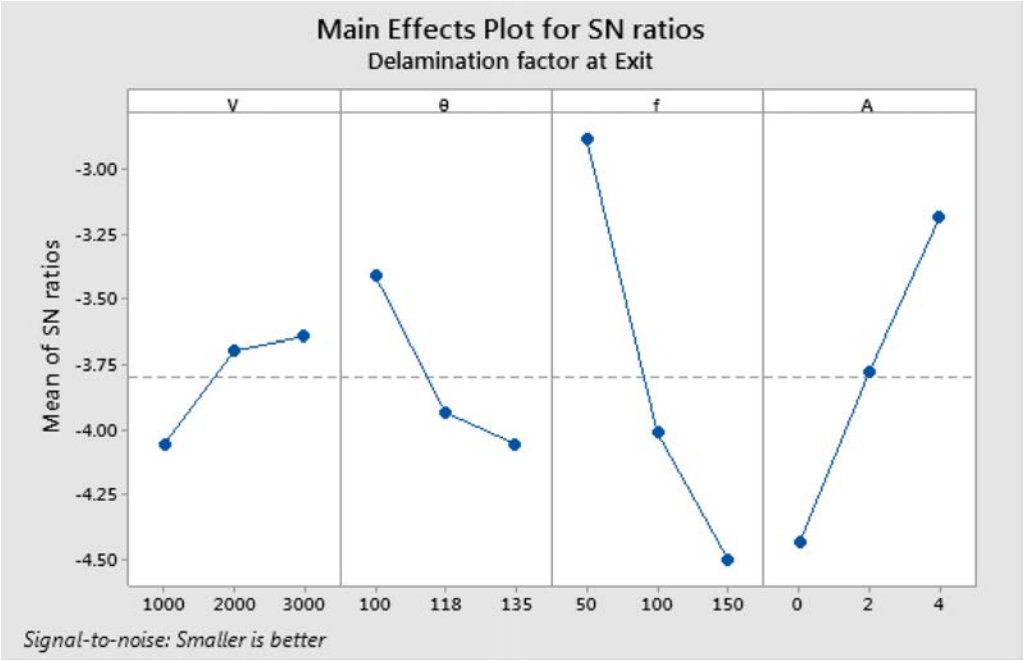

Fig. 5. S/N ratio plot for D-Exit.

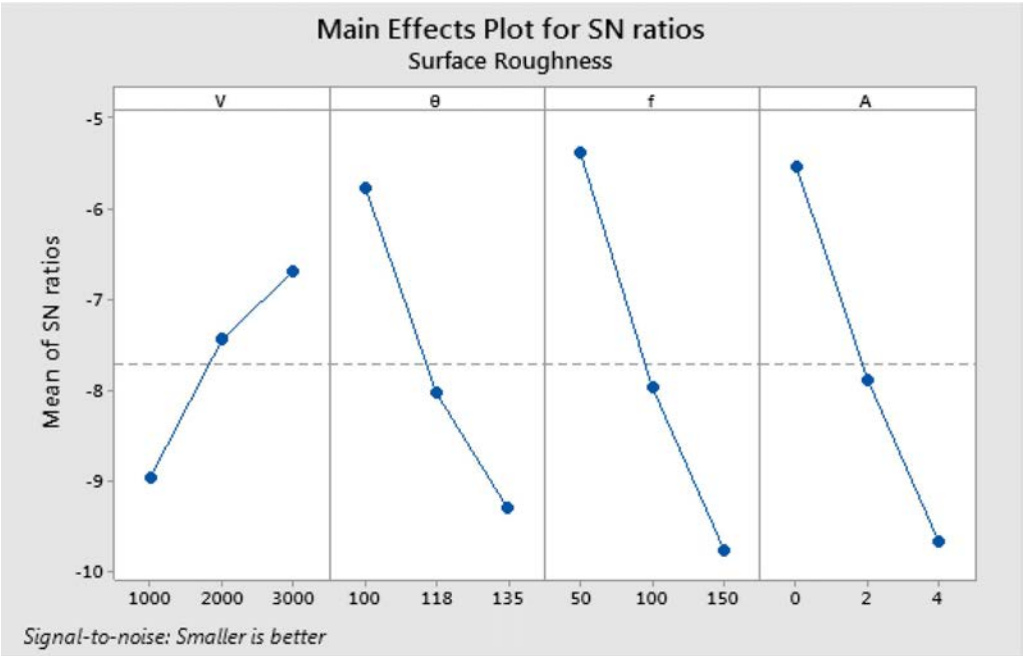

Fig. 6. S/N ratio plot for Ra.

The feed has the highest influence on in D-exit (49.36) followed by reinforcement wt.%. Feed rate has maximum influence on Ra (33. 92%) followed by reinforcement wt.%. Reinforcement wt. % has utmost influence on F (52%) followed by point angle. As the strength of the composite increases with the increase of wt% of Al_2O_3, more force is required to drill them, hence the increase in the thrust force. Among the drilling parameters considered, spindle speed is the least influencing factor.

From Table 11, it is obvious that R^2 values are almost closer to unity and the deviation with adj. R^2 is also least which indicates the importance of the developed model.

The second order quadratic regression models for D-entry, d-exit, surface roughness and thrust force were developed through RSM [26, 29]. Additionally, ANOVA for the output response are shown in Tables 12, 13, 14 and 15. Based on the results obtained from the drilling

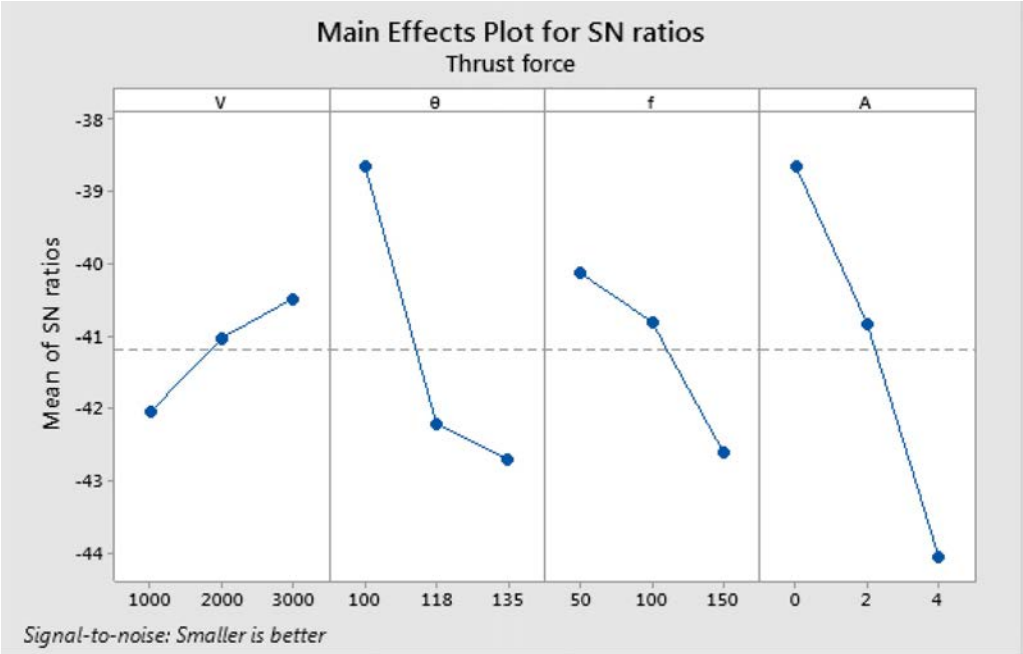

Fig. 7. S/N ratio plot for thrust force.

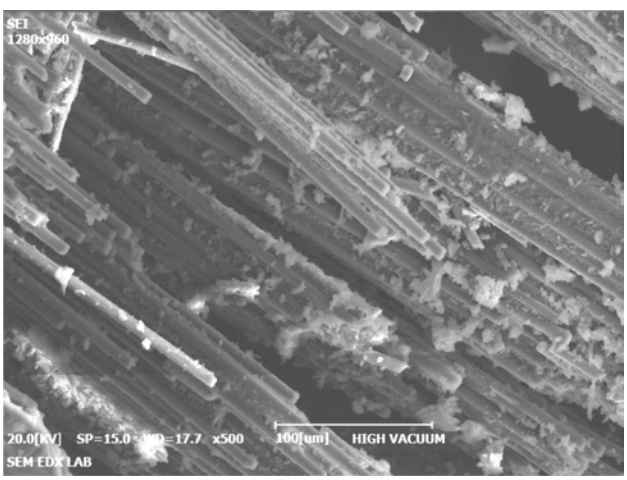

Fig. 8. SEM micrograph of drilled surface.

operations conducted on CFRP composites the equations obtained for D-entry, D-exit, Ra and F depending on the input parameters are as follows.

Delamination factor at Entry

$$= 2.268 + 0.000002\ V - 0.02919\ \theta - 0.00209\ f + 0.1328\ A - 0.000000\ V*V + 0.000114\ \theta*\theta + 0.000004\ f*f - 0.01020\ A*A + 0.000000\ V*\theta + 0.000000\ V*f + 0.000017\ V*A - 0.000012\ \theta*f + 0.000083\ \theta*A + 0.000138\ f*A \quad (6)$$

Delamination factor at Exit

$$= -0.61 - 0.000173\ V + 0.0298\ \theta + 0.00525\ f + 0.1119\ A + 0.000000\ V*V - 0.000108\ \theta*\theta - 0.000022\ f*f + 0.00287\ A*A + 0.000000\ V*\theta + 0.000001\ V*f - 0.000009\ V*A + 0.000011\ \theta*f - 0.001163\ \theta*A - 0.000259\ f*A \quad (7)$$

$$\mathbf{Ra} = -6.07 - 0.00038\ V + 0.127\ \theta - 0.0199\ f + 0.357\ A + 0.000000\ V*V - 0.000526\ \theta*\theta - 0.000004\ f*f - 0.0204\ A*A - 0.000001\ V*\theta - 0.000003\ V*f - 0.000032\ V*A + 0.000304\ \theta*f - 0.00165\ \theta*A + 0.00274\ f*A \quad (8)$$

Thrust force

$$= -692 - 0.0209\ V + 13.58\ \theta - 1.246\ f - 21.33\ A + 0.000004\ V*V - 0.05681\ \theta*\theta + 0.003825\ f*f + 3.151\ A*A + 0.000024\ V*\theta - 0.000019\ V*f - 0.004319\ V*A + 0.00675\ \theta*f + 0.2817\ \theta*A + 0.0342\ f*A \quad (9)$$

R^2 and predicted R^2 values of the second order quadratic models are: D-entry (R^2 = 99.69% & R^2 (pred) = 99.31%), D-exit (R-Sq = 94.81% & R-Sq (pred) = 88.76%), Ra (R^2= 92.00% & R^2 (pred) = 82.66%), Ra (R^2= 99.24% & R^2 (pred) = 94.79%). Deviation between R^2 and predicted R^2 is negligible (within 5%) for each regression model enlightens for precise prediction capability of the constructed models.

Tensile and flexural test

It is obvious from Fig. 9 that with an increase in wt% of alumina in the epoxy matrix, the tensile strength (TS) increases up to a maximum value and decreases consequently for higher concentration due to the agglomerations of nanoparticles [27]. It is observed that CFRP composite with 2% Al_2O_3 revealed more TS compared to others.

Table 11. ANOVA for D-Entry, D-Exit, Ra and F

Source	DF	Adj SS	Adj MS	F-Value	P-Value	% of Contribution
Delamination factor at Entry (R-Sq =98.82%, R-Sq (adj) =98.29%)						
V	2	0.04444	0.022222	17.50	0.000	2.30
θ	2	0.05719	0.028595	22.52	0.000	2.97
f	2	0.16640	0.083199	65.53	0.000	8.63
A	2	1.63860	0.819300	645.26	0.000	84.92
Error	18	0.02285	0.001270			1.18
Total	26	1.92949				100
Delamination factor at Exit (R-Sq =91.47%, R-Sq (adj) =87.68%)						
V	2	0.02660	0.013301	3.57	0.049	3.39
θ	2	0.06990	0.034951	9.39	0.002	8.90
f	2	0.38752	0.193760	52.06	0.000	49.36
A	2	0.23413	0.117063	31.45	0.000	29.82
Error	18	0.06699	0.003722			8.53
Total	26	0.78514				100.00
Surface Roughness Ra = (R-Sq =94.10%, R-Sq (adj) =87.03%)						
V	2	2.133	1.0664	4.72	0.023	8.33
θ	2	4.555	2.2773	10.07	0.001	17.80
f	2	8.681	4.3406	19.20	0.000	33.92
A	2	6.153	3.0767	13.61	0.000	24.04
Error	18	4.069	0.2261			15.90
Total	26	25.591				100.00
Thrust force F = (R-Sq =95.60%, R-Sq (adj) =93.64%)						
V	2	2428	1213.8	9.38	0.002	4.59
θ	2	14743	7371.5	56.99	0.000	27.88
f	2	5880	2939.8	22.73	0.000	11.12
A	2	27494	13747.2	106.28	0.000	52.00
Error	18	2328	129.4			4.40
Total	26	52873				100.00

Table 12. ANOVA for D-entry

Source	DF	Adj SS	Adj MS	F-Value	P-Value
Model	14	1.92342	0.13739	271.60	0.000
Linear	4	1.88631	0.47158	932.25	0.000
V	1	0.04377	0.04377	86.53	0.000
θ	1’	0.04926	0.04926	97.38	0.000
f	1	0.16526	0.16526	326.69	0.000
A	1	1.62802	1.62802	3218.38	0.000
Square	4	0.01862	0.00465	9.20	0.001
V*V	1	0.00059	0.00059	1.17	0.301
θ*θ	1	0.00729	0.00729	14.41	0.003
f*f	1	0.00075	0.00075	1.49	0.246
A*A	1	0.00998	0.00998	19.74	0.001
2-Way Interaction	6	0.01678	0.00280	5.53	0.006
V*θ	1	0.00017	0.00017	0.35	0.567
V*f	1	0.00119	0.00119	2.34	0.152
V*A	1	0.01094	0.01094	21.63	0.001
θ*f	1	0.00106	0.00106	2.10	0.173
θ*A	1	0.00008	0.00008	0.15	0.705
f*A	1	0.00171	0.00171	3.38	0.091
Error	12	0.00607	0.00051		
Total	26	1.92949			

Table 13. ANOVA for D-exit

Source	DF	Adj SS	Adj MS	F-Value	P-Value
Model	14	0.744400	0.053171	15.66	0.000
Linear	4	0.687412	0.171853	50.62	0.000
V	1	0.023716	0.023716	6.99	0.021
θ	1	0.062682	0.062682	18.46	0.001
f	1	0.369308	0.369308	108.77	0.000
A	1	0.231707	0.231707	68.25	0.000
Square	4	0.027884	0.006971	2.05	0.151
V*V	1	0.002898	0.002898	0.85	0.374
θ*θ	1	0.006533	0.006533	1.92	0.191
f*f	1	0.017662	0.017662	5.20	0.042
A*A	1	0.000790	0.000790	0.23	0.638
2-Way Interaction	6	0.026251	0.004375	1.29	0.333
V*θ	1	0.000015	0.000015	0.00	0.948
V*f	1	0.007483	0.007483	2.20	0.163
V*A	1	0.002752	0.002752	0.81	0.386
θ*f	1	0.000869	0.000869	0.26	0.622
θ*A	1	0.014927	0.014927	4.40	0.058
f*A	1	0.006060	0.006060	1.78	0.206
Error	12	0.040742	0.003395		
Total	26	0.785142			

Table 14. ANOVA for Ra

Source	DF	Adj SS	Adj MS	F-Value	P-Value
Model	14	23.5428	1.68163	9.85	0.000
Linear	4	21.1146	5.27864	30.93	0.000
V	1	2.0040	2.00401	11.74	0.005
θ	1	4.3709	4.37094	25.61	0.000
f	1	8.6158	8.61583	50.48	0.000
A	1	6.1238	6.12378	35.88	0.000
Square	4	0.3221	0.08052	0.47	0.756
V*V	1	0.1262	0.12615	0.74	0.407
θ*θ	1	0.1553	0.15533	0.91	0.359
f*f	1	0.0006	0.00060	0.00	0.954
A*A	1	0.0400	0.04002	0.23	0.637
2-Way Interaction	6	2.0208	0.33679	1.97	0.149
V*θ	1	0.0036	0.00362	0.02	0.887
V*f	1	0.2483	0.24831	1.45	0.251
V*A	1	0.0365	0.03654	0.21	0.652
θ*f	1	0.6359	0.63594	3.73	0.078
θ*A	1	0.0301	0.03009	0.18	0.682
f*A	1	0.6767	0.67672	3.96	0.070
Error	12	2.0482	0.17068		
Total	26	25.5910			

Table 15. ANOVA for F

Source	DF	Adj SS	Adj MS	F-Value	P-Value
Model	14	52472.3	3748.0	112.26	0.000
Linear	4	46787.2	11696.8	350.33	0.000
V	1	2317.5	2317.5	69.41	0.000
θ	1	12767.7	12767.7	382.41	0.000
f	1	5295.1	5295.1	158.59	0.000
A	1	26407.0	26407.0	790.92	0.000
Square	4	3425.7	856.4	25.65	0.000
V*V	1	111.4	111.4	3.34	0.093
θ*θ	1	1812.6	1812.6	54.29	0.000
f*f	1	548.8	548.8	16.44	0.002
A*A	1	953.0	953.0	28.54	0.000
2-Way Interaction	6	1927.7	321.3	9.62	0.001
V*θ	1	1.6	1.6	0.05	0.828
V*f	1	8.0	8.0	0.24	0.633
V*A	1	671.5	671.5	20.11	0.001
θ*f	1	313.9	313.9	9.40	0.010
θ*A	1	875.2	875.2	26.21	0.000
f*A	1	105.3	105.3	3.15	0.101
Error	12	400.7	33.4		
Total	26	52872.9			

The three point bend test is conducted on CFRP composite samples as per ASTM D790 standard. The size of the specimen was 200 mm ×12.7 mm × 3 mm with a length of 50 mm and 1.5 mm/min cross head-speed maintained for the test. It is obvious from Fig. 10 that with an increase in wt% of Al_2O_3 in the epoxy matrix, the flexural strength (FS) increases up to an inclusion of 2% concentration and gets reduced afterward

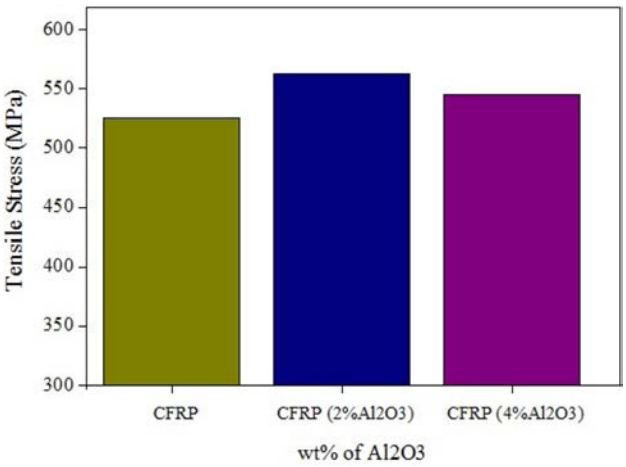

Fig. 9. TS with increase in wt% of Al_2O_3.

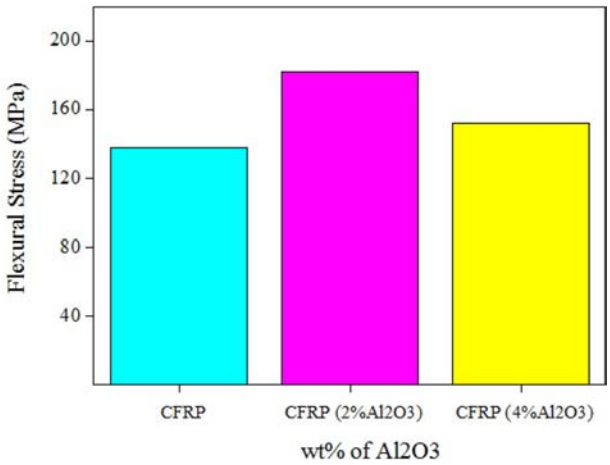

Fig. 10. FS with increase in wt% of Al_2O_3.

for 4 wt% of Al_2O_3 due to nanoparticle agglomerations. The enhanced FS was due to the better dispersion of Al_2O_3 nanoparticle in the epoxy matrix and at greater concentration, aggregation of Al_2O_3 naonoparticles occurs which decreases the FS of the composites [28].

Conclusions

CFRP composite was fabricated with the incorporation of Al_2O_3 particles through hand layup technique. The drilling tests were carried out on the basis of L27 OA and the optimal conditions were found for lowest delamination, surface roughness and thrust force. Second order quadratic models were developed for all responses through regression analysis.

The most influencing factor attained from GRA is feed rate followed by point angle whereas the reinforcement weight % shows least influence. The results of GRA show that spindle speed (3000rpm), point angle (100°), feed (50 mm/min) and reinforcement weight % (wt%4) of Al_2O_3 would lead to lowest value of D-entry, D-exit, Ra and F. The suggested optimum parameter

combination provides the outcome of 1.1469 D-entry, 1.2918 D-exit, 1.94 μm Ra and 95.29N thrust force. From ANOVA study, it can be concluded that reinforcement wt% (Al_2O_3) has the dominant effect on D-entry and thrust force whereas feed rate has significant effect on D-exit and Ra. The inclusion of up to 2 wt% concentration of Al_2O_3 in the composite increased both, the tensile and flexural strengths whereas further rise in concentration reduced the strengths due to nanoparticle agglomerations.

References

1. P.E. Faria, J.C. Campos Rubio, A.M. Abrao, and J.P. Davim, J. Reinf. Plast. Compos. 28[19] (2009) 2353-2363.
2. R. Stone and K. Krishnamurthy, Int. J. Mac. Tools. Manuf. 36[9] (1996) 985-1003.
3. L.M.P. Durao, D.J.S. Goncalves, J.M.R.S. Tavares, V.H.C. de Albuquerque, A.A. Vieria, and A.T. Marques, Comp. Struct. 92[7] (2010) 1545-1550.
4. B. Ravi Sankar, P. Umamaheswarrao, A.V. Avinash Reddy, and P. Koushik Kumar, J. Bas. App. Eng. Res. 1[3] (2014) 19-24
5. S.O. Ismail, H.N. Dhakal, I. Popov, and J. Beaugrand, Eng. Sci. Technol. Int. J. 19[4] (2016) 2043-2052.
6. Y. Turki, M. Habak, R. Velasco, Z. Aboura, K. Khellil, and P. Vantomme, Int. J. Mach. Tools. Manuf. 87 (2014) 61-72.
7. D.F. Liu, Y.J. Tang, and W.L. Cong, Compos. Struct. 94[4] (2012) 1265-1279.
8. R. Baptista, A. Mendao, M. Guedes, and R.M. Mendes, Procedia Struc Integrity 1 (2016) 74-81.
9. T. Rajmohan, Int. J. Part. Sci. Technol. 37[1] (2016) 21-30.
10. S.R. Ranganatha and V.S. Ramamurthy, Int. J. Adv. Eng. Technol. 4[3] (2013) 105-107.
11. V. Krishnaraj, A. Prabukarthi, A. Ramanathan, N. Elanghovan, M. Senthil Kumar, R. Zitoune, and J.P. Davim, Composites 43[4] (2012) 1791-1799.
12. H. Zhang, W. Chen, D. Chen, and L. Zhan, Key Eng. Mater. 196 (2001) 43-52.
13. U. Heisel and T. Pfeifroth, Proc CIRP 1 (2012) 471-476.
14. L.M.P. Durao, D.J.S. Goncalves, J.M.R.S. Tavares, V.H.C. Albuquerque, and A. de Torres Marques, in Proceedings of the 14th European conference on composite materials, June 2010, (Budapest University, 2010) p.1-10.
15. A. Krishnamoorthy, S. Rajendra Boopathy, K. Palanikumar, and J. Paulo Davim, Measurement 45[5] (2012) 1286-1296.
16. S. Aravind, K. Shunmugesh, J. Biju, and J.K. Vijayan, Mater. Today: Procee 4[2] (2017) 4188-4195.
17. K. Abhishek, S. Datta, and S.S. Mahapatra, Int. J. Adv. Manuf. Technol. 76[1-4] (2015) 401-416.
18. M.P. Jenarthanan and N. Naresh, Ind. J. Eng. Mat. Sci. 22 (2015) 313-320.
19. A. Noorul Haq, P. Marimuthu, and R. Jeyapaul, Int. J. Adv. Manuf. Technol. 37[3-4] (2008) 250-255.
20. R. Viswanathan, S. Ramesh, S. Maniraj, and V. Subburam, Measurement 159 (2020) 107800.
21. G. Anand, N. Alagumurthi, R. Elansezhian, K. Palanikumar, and N. Venkateshwaran, J. Braz. Soci. Mech. Sci. Eng. 40[4] (2018) 214.
22. W.C. Chen, Int. J. Mach. Tools. Manuf. 37[8] (1997) 1097-1108.
23. J. Lin and C. Lin, Int. J. Mach. Tools. Manuf. 42[2] (2002) 237-244.
24. D. Julong, J. Grey System 1[1] (1989) 1-24.
25. S. Ramesh, R. Viswanathan, and S. Ambika, Measurement, 78 (2016) 63-72.
26. R. Viswanathan, S. Ramesh, N. Elango, and D.K. Kumar, Pert. J. Sci. Technol. 25[1] (2017) 255-262.
27. H.B Kaybal, Hasan Ulus, and A.V.C Ahmet, Int. J. Inno. Res. Sci. Eng. Technol. 5[12] (2016) 75-79.
28. A. Mohanty and V.K. Srivastava, Fib. Poly. 16 [1] (2015) 188-195.
29. T. Pridhar, K. Ravikumar, B. Sureshbabu, R. Srinivasan, and B. Sathishkumar, Int. J. Ceram. Process. Res. 21[2] (2020) 131-142.
30. C. Chanakyan and S. Sivasankar, Int. J. Ceram. Process. Res. 21[6] (2020) 647-655.
31. Y.C. Lin, J.C. Hung, H.M. Chow, and A.C. Wang, Int. J. Ceram. Process. Res. 16[2] (2015) 249-257.